Vibrational Band Assignments for the Chiral Modifier Cinchonidine: Implications for Surface Studies

Wei Chu,[†] Rene J. LeBlanc, and Christopher T. Williams*

Department of Chemical Engineering, Swearingen Engineering Center, University of South Carolina, Columbia, South Carolina 29208

Jun Kubota[‡] and Francisco Zaera

Department of Chemistry, University of California, Riverside, California 92521

Received: July 7, 2003; In Final Form: September 24, 2003

Vibrational assignments for the chiral molecule cinchonidine using a combination of experimental vibrational spectroscopic measurements and ab initio computational methods are reported. Several bands in both the IR and Raman spectra are identified as useful in providing information regarding the mode of adsorption of cinchonidine on metal surfaces, a system of great relevance to enantioselective catalysis. In particular, vibrational modes associated with the quinoline group can be used to diagnose the degree of tilt of the molecule with respect to the plane of the substrate. The use of this information for the study of cinchonidine adsorption on polycrystalline platinum with both reflection−absorption infrared spectroscopy (RAIRS) and surface-enhanced Raman spectroscopy (SERS) is discussed. Adsorption geometries for cinchonidine on platinum at low and high concentrations are reported.

1. Introduction and Background

One of the more successful approaches for engendering enantioselectivity in heterogeneous catalysts involves modification of supported transition-metal catalysts by adsorption of chiral molecules during reaction.[1] In particular, the asymmetric hydrogenation of α-ketoesters over platinum catalysts modified by cinchona alkaloids has received much attention since its discovery by Orito in 1978.[2] These catalysts have been shown to be effective for performing enantioselective hydrogenation on a range of C═O bond-containing molecules, including ketoacids,[1] ketoesters,[1] ketoamides,[3] and ketoacetals.[4,5] Several excellent reviews are available on this subject.[1,6,7]

Many investigations have addressed the kinetics of asymmetric hydrogenation reactions catalyzed by cinchona alkaloid-modified transition metals.[1,6−11] However, there have been few surface-science investigations of this system. Two factors have contributed to this situation. The first and perhaps most problematic reason has been that the modification of catalyst surfaces with cinchona and the subsequent catalytic reactions both occur at a liquid−solid interface. This presents problems for the standard array of surface-science approaches used in a vacuum and gas-phase environments. The second reason is that the cinchona alkaloids are considerably more complex than the molecules typically examined with standard surface-science approaches. Figure 1 shows the structure of cinchonidine, the most common cinchona modifier used in chiral catalysis. The three main moieties of that molecule are highlighted, namely, an aromatic quinoline, a tertiary nitrogen-containing quinuclidine, and a linking chiral hydroxyl center.

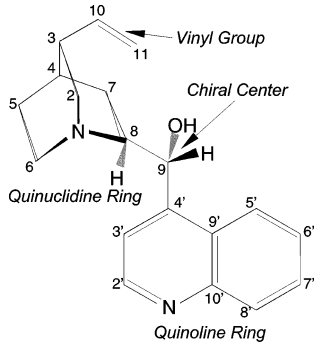

Figure 1. Structure of cinchonidine.

Notwithstanding such hurdles, a few surface-science investigations of this system have been reported in the literature. For one, Wells and co-workers have examined modified single crystalline Pt surfaces in ultrahigh vacuum using X-ray photoelectron spectroscopy (XPS) and low-energy electron diffraction (LEED).[12] Lambert et al. have characterized the adsorption of similar modifiers by XPS, temperature programmed desorption (TPD), near-edge absorption fine structure spectroscopy (NEXAFS), and scanning tunneling microscopy (STM).[13] Xu et al. have recently examined cinchonidine adsorption on Cu(111) in an electrochemical environment using STM.[14] More to the point of this report, three groups have examined the adsorption of cinchonidine on platinum in situ using vibrational spectroscopy. Kubota and Zaera have characterized the adsorption of cinchonidine on polycrystalline Pt surfaces from CCl_4 solutions using reflection−absorption infrared spectroscopy (RAIRS).[15−18] Ferri and co-workers have studied cinchonidine adsorption on model Pt/Al_2O_3 and Pd/Al_2O_3 surfaces using attenuated total reflection infrared spectroscopy (ATR−

* To whom correspondence should be addressed. Fax: (803)777-8265. E-mail: willia84@engr.sc.edu.

[†] Present address: Center for Marine Materials, Florida Atlantic University−SeaTech Campus, 101 North Beach Road, Dania Beach, FL 33004.

[‡] Present address: Chemical Resources Laboratory, Tokyo Institute of Technology, 4259 Nagatsuda Midoriku, Yokohama 226-8503, Japan.

10.1021/jp0359586 CCC: $25.00
Published on Web 11/25/2003

IRS).[19−21] Finally, Chu et al. have examined adsorption of cinchonidine on polycrystalline Pt surfaces in ethanol using surface-enhanced Raman spectroscopy (SERS).[22,23] Taken together, these spectroscopic results suggest that the cinchonidine binds to platinum through the quinoline group, with a degree of tilt with respect to the surface that increases with increasing solution concentration.

To interpret vibrational spectroscopic data for cinchonidine on various metal surfaces, a thorough understanding of the vibrational features of this modifier is required. However, the relative complexity of the cinchonidine molecule makes interpretation of even bulk-phase vibrational data a considerable challenge. Cinchonidine has 126 normal vibrational modes, and because the molecule is chiral, all of these vibrations are in principle *both* infrared and Raman active. It is perhaps unsurprising that a full set of vibrational band assignments of this molecule is not available. A few vibrational bands can be readily assigned using characteristic frequency tables.[24,25] A limited number of modes have also been identified in Raman spectroscopy experiments,[26] and some surface spectroscopic studies report vibrational band assignments[15,20,22] for solid cinchonidine based on ab initio quantum mechanics calculations involving Hartree−Fock or density functional theory (DFT) approaches. Overall, though, the vibrational information on cinchonidine available to date is very limited.

In this paper we present a comprehensive set of vibrational band assignments for solid cinchonidine. The band assignments have been made with the aid of both density functional theory and Hartree−Fock calculations as well as by more traditional methods such as characteristic frequency tables and comparison with spectra of related molecules. Particular emphasis has been placed on those bands that are expected to be important for surface studies, with specific examples culled from our recent research in this area. Nevertheless, our report is also expected to have a more extended impact in other areas of research, especially because cinchona alkaloids are one group of "privileged" chemicals with a wide range of applications in chiral synthesis.[27]

2. Experimental Section

Raman and Infrared Spectroscopy. A LabRam confocal Raman spectrometer (JY Horiba) was used for all Raman and SERS measurements discussed herein. The spectrometer is equipped with a liquid-nitrogen cooled, charged coupled device (CCD) detector, and a HeNe (632.817 nm) laser for excitation. The preparation method used for SERS-active platinum substrates and the details of the liquid cell used for all in situ SERS measurements have been described elsewhere.[22] The infrared data have been obtained by using a commercial Mattson Sirius 100 Fourier transform IR spectrometer and a narrow-band MCT detector. IR spectra for the bulk cinchona and related compounds reported here were obtained in the transmission mode, using KBr-diluted pellets for the solids and thin films pressed between NaCl disks for the liquids. In situ RAIRS experiments to characterize the adsorption of cinchonidine from liquid solutions onto platinum surfaces were carried out by using a cell described in detail elsewhere.[16,17] The PeakSolve windows-based software was used to fit and deconvolute both Raman and IR spectra. Unless otherwise noted, Lorentzian line shapes were used to fit all of the peaks.

Computational Methods. Ab initio quantum mechanics calculations were carried out using the Gaussian 98/98W suite of programs.[28] Density functional theory (DFT) calculations were performed using the B3PW91 method, which is a combination of Becke's three-parameter exchange functional[29] and the correlation functional of Perdew and Wang,[30,31] and the LANL2DZ basis set.[32−34] It is well-known that DFT methods overestimate the frequency of molecular modes, typically by around 1−5%,[35] so, in lieu of published scale factors for the B3PW91/LANL2DZ combination, a calibration procedure was developed. Using readily assigned vinyl and quinoline ring C═C stretching modes in cinchonidine (vide infra), frequency scale factors were fit for below (0.9657) and above (0.9431) 1800 cm^{-1}, as has been previously suggested by Halls and coworkers.[36] Similar scale factors were found to provide excellent results in calculations for the vibrations of quinoline as well (results not shown). The Hartree−Fock calculations were performed using a commercial Spartan RHF package and a 6-31G* basis set, and the results were scaled by the reported 0.8929 factor reported in the literature.[37] In all cases, the structure of cinchonidine was first optimized using the desired level of theory prior to performing vibrational frequency calculations. The vibrations were visualized using a combination of GaussView,[28] Molden,[38] and MacMolPlt[39] software packages.

3. Results and Discussion

The assignment of the vibrational spectra of cinchonidine was approached in the following fashion. First, a complete list of vibrational frequencies for solid cinchonidine was obtained by fitting the experimentally obtained Raman and IR spectra. Second, those data were compared to bulk spectra of structurally related compounds to identify peaks related to different functionalities within the modifier. Third, as many of the cinchonidine peaks as possible were assigned via consultation with characteristic frequency tables. Finally, quantum chemical calculations were performed at varying levels of theory on several different structures of cinchonidine to both confirm previous band assignments and assign the remaining vibrational modes. The following sections discuss this band assignment process in more detail. As reference during the discussion, the reader is directed to Table 1, which presents a summary of our vibrational mode assignments.

The middle traces in Figures 2 and 3 show the Raman and IR spectra for bulk cinchonidine, respectively. They point to the complexity of the vibrational spectra of cinchonidine. Besides a large number of overlapping peaks, many combination bands not related to individual vibrations are apparent as well. To compile a comprehensive list of peaks for assignment, each spectrum of cinchonidine was fitted using a series of individual peaks. By combining the fitted peak information from both Raman and infrared data, we generated a complete list of fundamental vibrational peaks. A partial list of these frequencies, which includes those that will be relevant for surface studies, is provided in Table 1.

Prior to making specific band assignments, comparisons were made with the spectra of several related or fragment molecules. In particular, the spectra of lepidine (bottom) and quinuclidine (top) were included in Figures 2 and 3 for comparison: lepidine is a good model for the aromatic portion of cinchonidine, whereas quinuclidine provides a good model for the portion containing the tertiary nitrogen, albeit without the vinyl group. In addition, the spectra of quinoline (a fragment), and dihydrocinchonidine (cinchonidine with the vinyl group hydrogenated), along with those of the structurally related quinine and dihydroquinine, were considered (Figure 4). Although certain vibrations are unique to the overall cinchonidine molecule, many bands are expected to easily identify with specific modes in moieties common to similar compounds. For example, Figures

TABLE 1: Vibrational Band Assignments for Solid Cinchonidine

experimental vibrational frequencies[a]		DFT[b] and Hartree−Fock[c] calculations for different molecular conformations[d]			
Raman (cm^{-1})	IR (cm^{-1})	open A2 DFT (cm^{-1})	open A1 DFT (cm^{-1})	open B1 RHF (cm^{-1})	description of vibrational mode[n]
		In the 700−1350 cm^{-1} Region			
758 (m)	nm	759	767	754	Q C−H oop wag + small QN def[e,f,l]
779 (m)	nm	777	776	782	Q C−H oop wag + small QN def[e−g,l]
804 (w)	804 (m)	796	803	796	QB C−H oop wag + Q OP def + QN def
884 (vw)	884 (m)	892	891	881	Q C−H op wag + small Q oop def
901 (vw)	901 (s)	917	908	895	Q C−H oop wag + QN def
1003 (vw)	1003 (m)	1004	1003	1006	QB CH oop wag
	1011 (w)	1011	1010	1015	vinyl CH_2 torsion + Q ip ring def
1025 (w)	1025 (w)	1013	1010	1022	vinyl CH_2 torsion + very small Q ip ring def
1037 (w)	1037 (w)	1031	1041	1030	50% Q ip def + 50% QN def
1059 (w)		1061	1058	1055	QN C−N−C & C−C−C str[e]
1098 (w)	1098 (vs)	1124	1120	1100	QN CH_2 rock, CH wag, and OH bend[e]
1132 (vw)	1132 (w)	1134	1138	1128	Q CH ip bend + OH bend[f,i]
1163 (vw)	1163 (m)	1164	1168	1155	QB C−H ip bend. + QN CH_2 wag/rock[f,g]
1207 (vw)	1207 (w)	1213	1215	1212	QN CH_2 torsion and wag + Q C−H ip bend[e,g]
1281 (w)	1277 (w)	1287	1292	1291	vinyl C−H rock[l]
1302 (w)	1306 (w)	1299	1302	1302	QN CH and CH_2 wag[e]
1326 (vw)	1326 (w)	1320	1320	1323	QB ip ring def + QN CH_2 wag[e]
1336 (vw)	1336 (w)	1321	1326	1334	QN CH wag + Q CNC and CCC A stretch[e]
		In the 1350−1700 cm^{-1} and 2800−3100 cm^{-1} Regions			
	1356 (w)	1342	1338	1355	vinyl C=C−C def[l,m]
1361 (vs)		1362	1353	1363	Q ring stretch and CH ip bend + QN CH wag[f−i]
1366 (vs)	1366 (w)	1374	1364		Q ring stretch and CH ip bend + QN CH wag[f−i]
1383 (w)	1383 (m)	1384	1376	1381	Q ring stretch and CH ip bend[f−k]
1423 (m)	1423 (w)	1425	1423	1417	Q ip ring def[l,m]
1448 (vw)	1448 (vw)	1465	1465	1466	QN CH_2 oop scissor[l]
1453 (vw)	1453 (m)	1469	1468	1475	QN CH_2 oop scissor[e,k,l]
1463 (w)	1463 (w)	1478	1475	1478	QN CH_2 oop scissors[i−l]
1508 (vw)	1508 (m)	1508	1508	1506	Q ip ring def + Q C−H ip bend[f−k]
1569 (w)	1569 (m)	1559	1558	1603	Q ip ring def + Q C−H ip bend[f,h−k]
1591 (w)	1591 (m)	1592	1587	1619	Q ip ring def + Q C−H ip bend[f−k]
1617 (vw)	1617 (w)	1623	1623	1634	QB ip ring def + Q C−H ip bend[f−k]
1637 (w)	1637 (m)	1648	1648	1674	QN vinyl C=C stretch[j−l]
3070 (vw)		3069	3071	3038	QB C−H's stretches[l]
3074 (vw)	3074 (w)	3082	3084	3039	vinyl A C−H stretch[l]
3086 (vw)	3086 (vw)	3086	3074	3079	QP C−H stretch[l]

[a] The following letters describe the strengths of vibrational bands relative to the most intense band in the spectrum: vw, <5%; w, 6−25%; m, 26−75%; s, 76−95%; vs, 96−100%; nm, not measured. [b] DFT calculations performed using the B3PW91 method with the LANL2DZ basis set. See text for details. [c] RHF calculations performed using the 6-31G* basis set. See text for details. [d] Conformations as described in ref 48. [e] Supported by comparison with bulk Raman and IR spectra of quinuclidine (cf. Figures 2 and 3). [f] Supported by comparison with bulk Raman and IR spectra of lepidine and quinoline (cf. Figures 2 and 3). [g] Consistent with published band assignments for 2,2′-biquinoline (see ref 67). [h] Consistent with published band assignments for lepidine (see ref 55). [i] Consistent with published band assignments for monosubstituted quinolines (see ref 44). [j] Consistent with published band assignments for cinchonine (see ref 26). [k] Consistent with published band assignments for cinchonidine (see ref 20). [l] Consistent withcharacteristic frequency tables in refs 24 and 25. [m] Assigned by comparison of cinchonidine and dihydrocinchonidine spectra (cf. Figure 4). [n] Cinchonidine vibrational mode description using the following notation: Q = quinoline group, QB = benzene part of quinoline group, QP = pyridine part of quinoline group, QN = quinuclidine group, ip = in-plane, oop = out-of-plane, A = asymmetric, def = deformation, stretch = stetching, bend = bending, torsion = torsion, wag = wagging, rock = rocking.

2 and 3 reveal several clear similarities between cinchonidine and its fragments, lepidine and quinuclidine, in particular in the regions indicated by the dashed boxes. In this fashion it was possible to make some general band assignments for cinchonidine. For instance, the frequency regions between 1400 and 1700 cm^{-1} are almost identical in cinchonidine and lepidine. As such, most of the prominent bands in that region can be assigned to modes associated with the aromatic portion of cinchonidine. Similarly, comparisons between the three spectra in the C−H stretching region (2800−3100 cm^{-1}) suggest that quinuclidine-related bands in cinchonidine reside below 3000 cm^{-1}, whereas bands associated with the aromatic ring are above 3000 cm^{-1}. Table 1 indicates, when relevant, the comparisons to spectra of related molecules that support the band assignments listed.

Several of these fragment-specific band assignments were further specified by consultation with readily available Raman and IR characteristic frequency tables[24,25] and with previously reported band assignments. The band at 1637 cm^{-1} was readily assigned this way to the vinyl C=C stretching mode. Similarly, the peaks at 2975 and 3003 cm^{-1} (not listed in Table 1) were assigned to CH_2-related C−H stretches within the vinyl group, and the 3074 cm^{-1} band to the lone C−H stretch. In the case of quinuclidine, the cluster of bands at 1448, 1453, and 1463 cm^{-1} can be confidently assigned to CH_2 scissoring vibrations. Several of the aromatic-related vibrational bands were confirmed as well. In particular, the three bands at 1569, 1591, and 1617 cm^{-1} are consistent with reported C=C ring deformation vibrations of quinoline, whereas the prominent bands at 758 and 779 cm^{-1} in the Raman spectrum are consistent with the out-of-plane wagging vibrations of four adjacent aromatic hydrogens. It is important to note that previous vibrational studies of cinchonidine and related molecules have relied on consultation of only a few primary literature sources. For quinoline, the original comprehensive band assignments by Wait and McNerney[40] have been recently confirmed by quantum

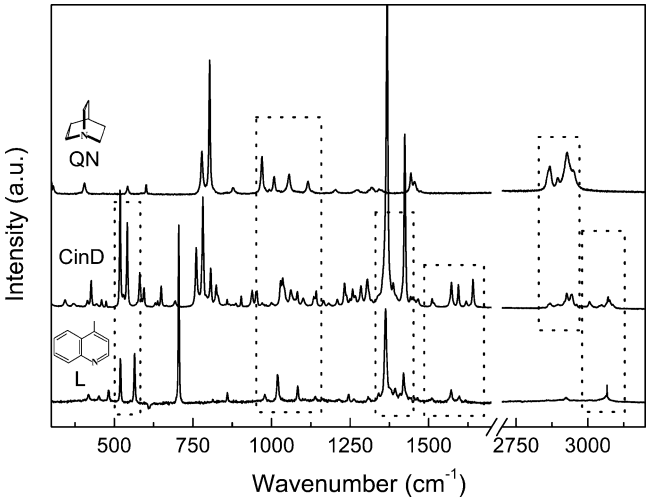

Figure 2. Comparison of Raman spectra of cinchonidine (CinD), lepidine (L), and quinuclidine (QN) at room temperature. The dotted boxes indicate similarities between the spectra.

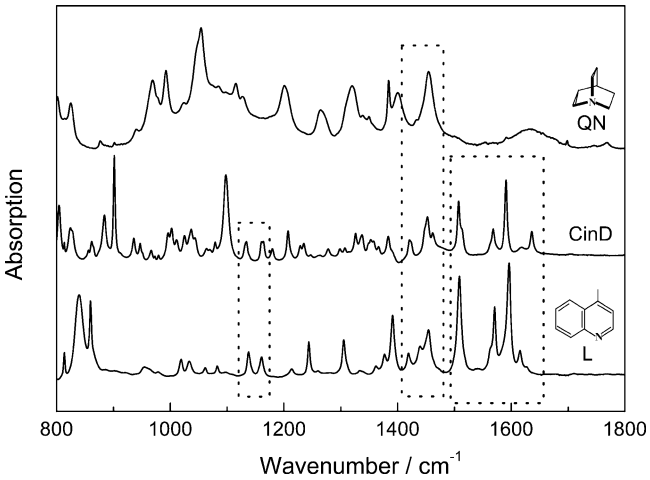

Figure 3. Comparison of infrared spectra of cinchonidine (CinD), lepidine (L), and quinuclidine (QN) at room temperature. The dotted boxes indicate similarities between the spectra.

chemical calculations.[41] In the case of quinuclidine, the early papers by Bruesch and co-workers[42,43] are still the standard references. Katritzky and Jones[44] have compared and assigned the vibrational spectra of a series of monosubstituted quinolines. Table 1 indicates when this primary literature or the characteristic frequency tables support a given band assignment.

Once our preliminary band assignments were completed, quantum chemical calculations of vibrational frequencies were performed. The goal was to develop a more complete picture of the vibrational modes of this complex molecule. But first, a decision had to be made regarding the conformation of cinchonidine that should be used. Molecular simulation studies have indicated that there are several conformers of cinchonidine that exhibit local energy minima,[45−49] with most recent estimates being as high as nine.[48,49] Similar results (not shown) were found here from calculations using the PM3[50,51] semiempirical approach. The structures for cinchonidine can be divided into two classes, typically characterized as "open" and "closed". The six "open" conformers (designated as A1−A3 and B1−B3 in ref 48) are those in which the tertiary nitrogen on the quinuclidine group is pointed away from the nitrogen on the quinoline group. The three "closed" conformers (designated as C1−C3 in ref 48) are those in which the quinuclidine nitrogen is pointed toward the quinoline nitrogen and the aromatic ring.

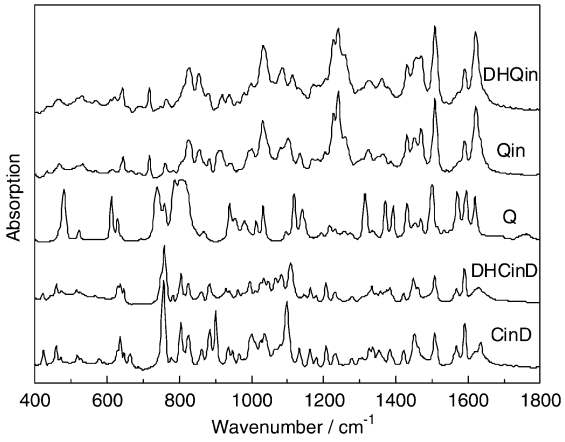

Figure 4. Comparison of infrared spectra of cinchonidine (CinD), dihydrocinchonidine (DHCinD), quinoline (Q), quinine (Qin), and dihydroquinine (DHQin).

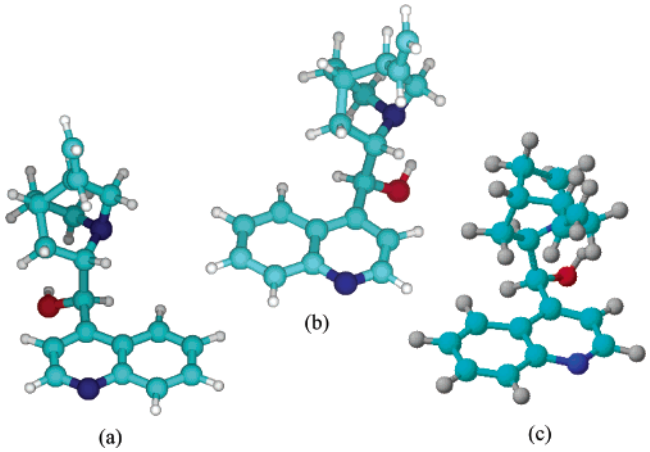

Figure 5. Ball and stick representations of the (a) A2, (b) A1, and (c) B1 conformations of cinchonidine used for calculating vibrational frequencies. Key: light blue = carbon, dark blue = nitrogen, red = oxygen, gray/white = hydrogen.

The structure of solid cinchonidine, shown in Figure 5a, has been clearly identified by X-ray diffraction[52] as the A2 structure of Margifalvi and Tfirst.[48] That structure was therefore chosen here as the primary basis for our DFT calculations of the vibrational modes of solid cinchonidine. Nevertheless, it is recognized that cinchonidine is likely to undergo conformation changes when in solution and when adsorbed on the surface of solid catalysts. Indeed, previous studies on the structural changes of cinchonidine as a function of solvent[47] have indicated that although the "open" A2 structure is still likely to be the most stable in many solutions, two "closed" conformations appear to become more stable in polar environments. It is therefore useful to also gain an understanding on the relative importance of conformation as it relates to the vibrational properties of cinchonidine. With this in mind, a second structure was chosen in our DFT studies for comparison, the "open" conformer designated A1 by ref 48 and shown in Figure 5b. A third structure, shown in Figure 5c (closer to structure B1 in ref 48), was used for the Hartree−Fock calculations. By using structures A1, A2, and B1, the effect of variations in the two main dihedral angles in the group linking the quinoline and quinuclidine groups could be explored. It should be said that most vibrational modes, in particular those localized or with high frequencies, are expected to be fairly insensitive to the structural details of the molecule, and that is in general what was found in our

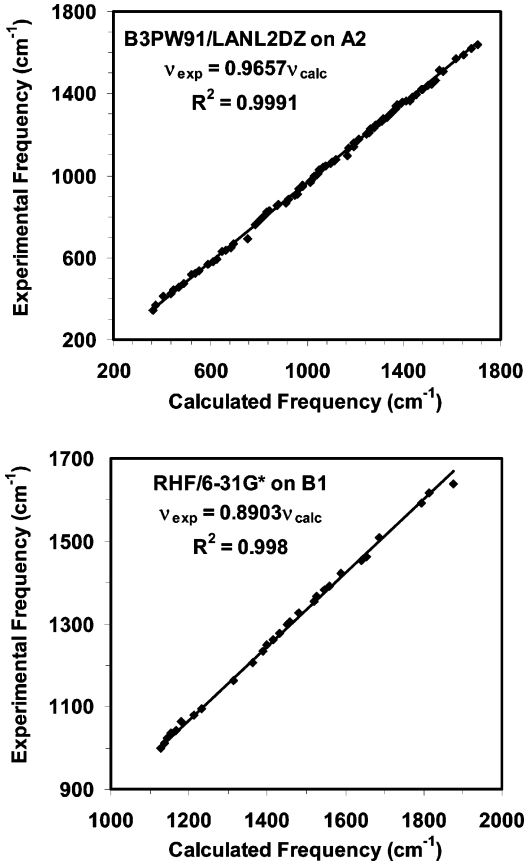

Figure 6. Plots of the calculated versus experimental frequencies for the A2 conformation calculated by B3PW91/LANL2DZ (top) and B1 conformation calculated by RHF/6-31G* (bottom).

calculations, especially for the vibrations associated with the quinoline group.

Following geometry optimization of each structure, vibrational frequencies were calculated to compare them with those obtained experimentally. For this study, we present the frequencies calculated for the A1 and A2 structures using B3PW91/LANL2DZ and for the B1 structure using RHF/6-31G*. By matching up the pre-assigned experimental peaks discussed above with the corresponding calculated vibrational modes, we could effectively align both lists of frequencies. Figure 6 shows plots of the calculated versus experimental frequencies for the A2 and B1 structures for the frequency region below 1800 cm^{-1} (similar plots were also produced for the C−H stretching region but are not shown here). As stated before, these calculations can overestimate the vibrational frequencies by up to ca. 10%.[35] However, thanks to the good linear relationships between the two sets of frequencies, the calculated frequencies could be easily scaled to compare to the experimental data. As can be seen in Table 1, the calculated frequencies after scaling are in excellent agreement with the experimental frequencies: the average root-mean-square error between the (scaled) calculated and experimental frequencies is around 10 cm^{-1} for both methods, well within the accuracy expected for this level of theory.[35,53] It is also encouraging to see that the scaling factor for the Hartree−Fock calculations deviates by less than 0.3% from the reported value.[37]

Following the matching up of our calculated frequencies with the experimental data, the peaks were assigned by examination of each vibrational mode using appropriate visualization software. The last column in Table 1 lists the descriptions of each vibrational mode. The results from the calculations lend further support to several of the vibrational assignments discussed above, and allow for several less straightforward assignments. For example, the prominent Raman peaks at 804, 884, 901, and 1003 cm^{-1} may now be confidently assigned as arising largely from C−H out-of-plane wagging on the quinoline group.

The present study is, to the best of our knowledge, the first ab initio quantum chemical study of the vibrational structure of cinchonidine. However, there have been several studies of related molecules reported in the literature. Weselucha-Birczynska and Nakamoto[54] used HF/STO-3G to predict and assign some of the vibrational modes of cinchonine as part of a Raman spectroscopic study. Ferri and Burgi[20] used B3PW91 with the triple-ζ version of Dunning's correlation-consistent basis set[55] to predict frequencies for quinoline and quinuclidine. A more recent DFT study has predicted vibrational frequencies for lepidine and isoquinoline using B3PW91/6-311G*.[56] Finally, Bandyopadhyay and Manogaran recently used HF/6-31G** to assign the vibrational spectra of quinoline and isoquinoline.[41] As indicated by Table 1, the results of our calculations (and hence our band assignments) appear to be largely in harmony with these related studies.

Additional information could be extracted from our calculations once the vibrational assignment was completed. In particular, the ability to visualize the vibrational modes of cinchonidine has made it possible to determine which modes arise purely from one functional group in the molecule, and which arise from a combination of groups. It was determined that most vibrational features in the 1500−1620 cm^{-1} energy range correspond exclusively to in-plane vibrational modes of the quinoline ring. On the other hand, it became clear that the out-of-plane C−H wagging vibrations lying between 700 and 900 cm^{-1} are in almost all cases convoluted with at least some contribution from deformations of the quinuclidine ring. Such mixing of vibrations from different parts of cinchonidine can complicate the analysis of surface vibrational spectra, which depends on surface selection rule arguments. In the case of infrared spectroscopy, it has been established that, on metal surfaces, only dynamic dipoles with a component perpendicular to the plane of the surface can be detected.[57,58] Appropriate visualization software was used here to calculate the vectorial coordinates of the dynamic dipole moment associated with each normal vibrational mode of the cinchonidine molecule, and that information was then used to determine adsorption geometries.[59] More details on interpretation of surface IR spectra as they relate to the cinchonidine system are given below. Surface-enhanced Raman spectroscopy has also been used extensively to study the adsorption mode of several different types of molecules. The selection rules for SERS have been presented previously[60−62] and also reviewed extensively.[63] SERS has been particularly effective for examining the adsorption of aromatic molecules onto metal surfaces, with the classic examples being pyridine, benzene, and related chemisorbates (see the discussions in ref 63). In many cases, and especially for transition metals,[64−66] orientation may be assessed by considering the relative enhancement of in plane versus out-of-plane vibrations, and by utilizing molecular symmetry arguments. However, unlike for IR at metal surfaces, the relevant parameter for Raman scattering is the change in the polarizability. Thus, some vibrations such as aromatic ring breathing modes that are parallel to the surface may exhibit significant Raman scattering. Perhaps most relevant to the current study, SERS selection rule arguments have been successfully used to analyze surface orientation of molecules having extended aromatic structures.[67−69]

In the next two sections we present a brief overview of some of our recent results using SERS and RAIRS to examine in

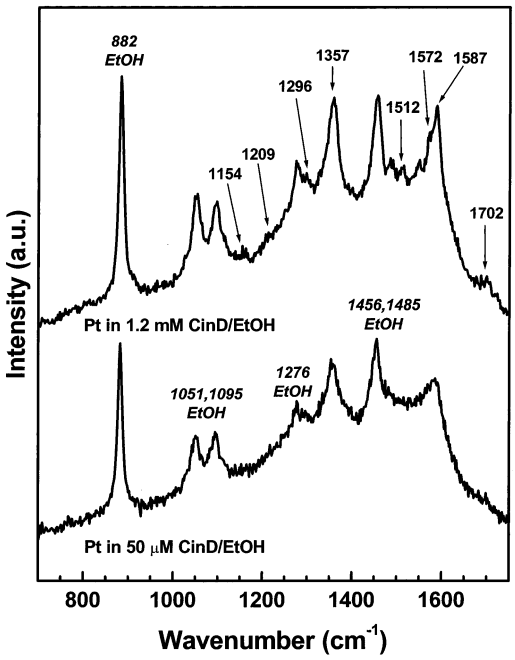

Figure 7. SERS data of Pt in 50 μM cinchonidine in ethanol (bottom) and 1.2 mM cinchonidine in ethanol (top). Arrows in the top spectrum refer to peaks that have become prominent as a result of raising the liquid-phase cinchonidine concentration. See Table 2 for band assignments.

situ the adsorption of cinchonidine from liquid solutions onto platinum surfaces. In both cases, emphasis is placed on how the vibrational data can be used to elucidate modes of adsorption and molecular orientations.

Figure 7 shows typical SER spectra acquired for platinum immersed in 50 μM (bottom spectrum) and 1.2 mM (top spectrum) ethanolic solutions of cinchonidine. The spectrum is complicated, and contains many overlapping peaks. The peaks at 882, 1051, 1095, 1276, and 1456 cm^{-1} are readily assigned to Raman scattering from bulk ethanol solvent. The presence of these peaks is expected, as the confocal collection optics cannot eliminate bulk-phase scattering completely. The remaining peaks in the spectrum arise from adsorbed cinchonidine, except for the broad humps that lay beneath the peaks between 1200 and 1700 cm^{-1}. These features are associated with trace amounts of carbonaceous impurities on the surface, as noted in many SERS investigations (see for example ref 70); the actual peak positions are typically at around 1580 and 1340 cm^{-1}, and are representative of graphitic and amorphous/disordered carbon, respectively.[71]

A list of band assignments for the cinchonidine surface peaks is provided in Table 2. The most prominent SERS peak is the one at 1357 cm^{-1}, which is assigned to a quinoline ring-stretching mode of cinchonidine adsorbed on Pt. The specific stretching involves the carbons located at the junction between the pyridine and benzene parts of the quinoline group (the C9′ and C10′ carbons in Figure 1). It is not surprising that this feature should be observed in the SER spectra, because it is the strongest vibration in the bulk Raman spectrum. The appearance of this feature offers an indication of the mode of adsorption on the surface. First, the width of the peak is broadened approximately 3-fold from its solid- and liquid-phase values, to 30 cm^{-1}. Second, the peak is red shifted ca. 10 cm^{-1} upon cinchonidine adsorption. By analogy with previous SERS investigation of aromatic adsorption onto transition metals,[64] both observations suggest that the quinoline group of the cinchonidine is π-bonded to the Pt surface. Indeed, the result

TABLE 2: SERS Vibrational Band Assignments for Cinchonidine/Pt in Ethanol

solid cinchonidine		on Pt	
Raman (cm^{-1})	calc A2 (cm^{-1})	SERS (cm^{-1})	description of vibrational mode
758 (m)	759	784 (w)	Q C−H oop wag + small QN def
779 (m)	777		Q C−H oop wag + small QN def
1163 (w)	1164	1154 (w)	QB C−H ip bend + QN CH_2 wag/rock
1207 (w)	1213	1209 (w)	QN CH_2 torsion and wag + Q C−H ip bend
1281 (w)	1287	1296 (w)	vinyl C−H rock
1302 (w)	1299		QN CH and CH_2 wag
1366 (vs)	1374	1357 (s)	Q ring stretch and CH ip bend + QN CH wag
1383 (w)	1384		Q ring stretch and CH ip bend
1508 (vw)	1508	1512 (m)	Q ip ring def + Q C−H ip bend
1569 (w)	1559	1572 (w)	Q ip ring def + Q C−H ip bend
1591 (w)	1592	1587 (m)	Q ip ring def + Q C−H ip bend
1617 (w)	1623	1613 (vw)	QB ip ring def + Q C−H ip bend
3086 (w)	3086	3089 (vw)	QP C−H stretch

is consistent with SERS measurements of quinoline on Pt (data not shown), which reveal a similar broadening and downshift in the associated ring-stretching mode. This strong interaction of the aromatic ring with the surface is consistent with what has been observed in other studies of this system.[12−23]

Examining the ratios of the peak intensities within the SER spectra makes possible a qualitative determination of the molecular orientation of the quinoline group.[63] The case of adsorption from the liquid phase containing 1.2 mM cinchonidine in Figure 7 is taken here as an example. Analysis of these SERS data suggests a significant tilt of the aromatic ring with respect to the surface, as indicated by the relative strengths of out-of-plane and in-plane vibrations within the quinoline ring structure. Unfortunately, the calculations reveal that there are not many pure out-of-plane aromatic vibrations in solid cinchonidine (i.e., they often include a contribution from the quinuclidine portion of the molecule), and, in addition, many such peaks are very weak Raman scatterers. Nevertheless, a broad feature in the SER spectra at ca. 784 cm^{-1} likely arises from a convolution of several largely out-of-plane C−H stretching vibrations on the aromatic ring (758 and 779 in the bulk Raman; see Table 1). There are several in-plane vibrations to choose from in the SER spectra, most notably the three peaks at 1512, 1572, and 1587 cm^{-1}, corresponding to the quinoline in-plane ring deformation modes at 1514, 1569, and 1591 cm^{-1}, respectively. When compared with the relative intensities of these bands in the normal Raman spectrum of pure cinchonidine (cf. Figure 2), it is clear that the set of in-plane vibrations in Figure 6 are enhanced considerably more upon adsorption than the out-of-plane vibrations. Thus, at a concentration of 1.2 mM it appears that the quinoline group is significantly tilted with respect to the Pt surface. It is interesting to note that at the lower concentration of 50 μM the in-plane vibrations are not as pronounced, indicating a flattening out of the aromatic ring with respect to the surface. Evidence for a tilt in the aromatic ring is also provided by the observation of a SERS peak at ca. 3089 cm^{-1} (not shown in Figure 7), corresponding to an in-plane C−H stretch of one of the two hydrogen atoms on the pyridine half of the quinoline group. Other cinchonidine C−H stretching vibrations are entirely covered up by those associated with ethanol, and therefore are not diagnostic under these conditions.

Similar conclusions can be reached from our RAIRS studies, which also provide more details about the adsorption geometry of cinchonidine. Figure 8 shows typical RAIRS traces in the 1150−1600 cm^{-1} wavenumber range for cinchonidine adsorbed on a platinum polycrystalline disk from 0.5 (bottom) and 1.2 mM (middle) carbon tetrachloride solutions. The top trace

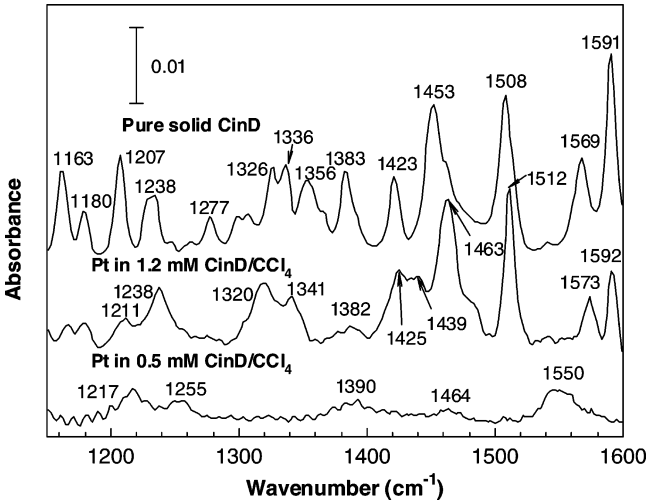

Figure 8. RAIRS data for Pt in 0.5 (bottom) and 1.2 (middle) mM cinchonidine solutions in carbon tetrachloride. The spectrum of pure cinchonidine is provided in the top trace for reference. See Table 3 for band assignments.

corresponds to pure cinchonidine in the solid phase and is provided for reference. Clearly, different spectra are obtained at low and high concentrations. Three regimes have in fact already been identified in this system: (1) no adsorption from solutions below 5% of saturation (saturation being 6.8 mM); (2) a flat geometry for concentrations between 5 and 20%; and (3) tilted configuration above 20%.[15] In addition, the adsorption geometry changes identified by IR were shown to correlate with the activity and selectivity variations reported for a similar system.[72] Here we expand on the interpretation of these RAIRS spectra in terms of the adsorption geometries that cinchonidine adopts upon adsorption from solution onto the platinum surface.

The RAIRS trace corresponding to cinchonidine adsorbed from the 0.5 mM CCl_4 solution displays five weak and broad features around 1217, 1255, 1390, 1464, and 1550 cm^{-1}. Some of these features may be due at least in part to interference from the solvent, because liquid carbon tetrachloride displays vibrations at 1217, 1252, and 1547 cm^{-1}. It is interesting to note, however, that the relative intensities of the two cases do not match: though the 1547 cm^{-1} band is significantly more intense than the other two in pure CCl_4, all three features have approximately the same cross section in the cinchonidine/Pt system. Moreover, the IR bands seen at low concentrations (the one around 1550 cm^{-1} in particular) are significantly reduced at higher concentrations. It is possible for some CCl_4 to be chemisorbed at low cinchonidine concentrations but to be displaced by the chiral modifier at higher concentrations. In any case, there are two features in the low-concentration IR trace, at 1390 and 1464 cm^{-1}, associated with a C8−C9 stretching and a quinuclidine C7 CH_2 scissoring mode, respectively (the numbers for the atoms refer to those in Figure 1). More telling is the absence of any of the intense peaks in the 1500−1600 cm^{-1} range due to in-plane quinoline deformations. This suggests an adsorption geometry for cinchonidine at low concentrations with a flat quinoline aromatic ring and the C8−C9 bond sticking out of the surface.

The spectra for cinchonidine adsorbed on platinum from high-concentration solutions are much richer in information. In particular, the intensities of infrared peaks associated with the quinoline in-plane vibrations in cinchonidine adsorbed on platinum as compared to solid cinchonidine provide information about the orientation of the ring with respect to the surface plane. In general, the large intensities of most of those peaks argue for a perpendicular, or at least highly tilted, geometry. In addition, because the dynamic dipole moments of the different modes have different orientations, they can be used to qualitatively determine the azimuthal angle of the quinoline ring with respect to the surface normal. Specifically, the peak at 1573 cm^{-1} corresponds to a compression/expansion of the ring along its short axis, and leads to a dynamic dipole oriented in that direction. The band at 1592 cm^{-1}, on the other hand, has a dynamic dipole approximately oriented along the N−C2′ bond. The relative increase in the intensity of the former with respect to the latter then argues for a rotation of the quinoline ring so the N−C2′ bond adopts an orientation close to parallel to the surface. This suggests an adsorption geometry through the quinoline nitrogen atom and with the adjacent benzene ring away from the surface.

The relative intensities of the other IR bands due to vibrations of the quinoline ring support this proposal. For one, the peaks at 1512, 1422, and 1238 cm^{-1}, which have dynamic dipoles oriented in directions close to that of the 1573 cm^{-1} feature, are also fairly intense. On the other hand, the peak at 1382 cm^{-1} is barely visible in the spectra of the adsorbed species. Because this vibrational mode has a dynamic dipole roughly oriented along the N−C10′ direction, its low intensity means that the quinoline plane must be somewhat tilted. Last, although significant frequency shifts are seen for vibrational modes where the nitrogen atom moves along the short axis of the quinoline ring (the 1573, 1512, and 1238 cm^{-1} peaks, corresponding to 1569, 1508, and 1233 cm^{-1} bands in solid cinchonidine), less changes are seen for the other ring deformation modes (the ones at 1592 and 1382 cm^{-1}, which have the same values, within experimental error, as in the solid). This provides evidence for a degree of σ bonding between the metal and one of the electron lone pairs of the nitrogen atom, again supporting the tilted geometry of the quinoline ring.

Analogous arguments can be made to estimate the orientation of the quinuclidine ring. In this case, the IR peaks at 1485 (a shoulder in the high energy of the 1453 cm^{-1} feature) and 1463 cm^{-1}, which increase in relative intensity upon cinchonidine adsorption on the platinum surface, can be identified with the C2 and C7 CH_2 scissoring modes, respectively, and have dynamic dipole moments perpendicular to the C2−C3−C7−C8 plane. On the other hand, the features at 1453 and 1448, due to C5 and in-phase combined C2+C5+C7 CH_2 deformations (both with dipoles parallel to the C2−C3−C7−C8 plane), virtually disappear. Also, the peak at 1211 cm^{-1} (1207 cm^{-1} in the solid), corresponding to an asymmetric combination of the torsion of the C5 and C6 CH_2 groups, shows low relative intensity, suggesting that the C5−C6 bond axis is also parallel to the surface. All these observations can be explained by a quinuclidine orientation where the C2−C3−C7−C8 plane is close to parallel to that of the metal surface. Finally, the lack of peaks for the skeletal deformation of the vinyl group at 1358 and 1281 cm^{-1} indicates that the C11−C10 plane must also be close to parallel to the platinum surface (actually, only the line bisecting the C11−C10−C3 angle needs to be parallel to the surface).

Finally, it is worth noticing the significant changes that occur in the 1300 to 1350 cm^{-1} of the IR spectra of cinchonidine upon adsorption on the platinum surface. Specifically, it can be seen that the features at 1326 and 1336 cm^{-1} for solid cinchonidine shift to 1320 and 1341 cm^{-1}, respectively, upon adsorption. These modes are associated with deformations in the quinuclidine ring close to the linkage to the chiral center, that is, with carbons C7, C8, and C9. There appears to be an

TABLE 3: RAIRS Vibrational Band Assignments for High-Coverage Cinchonidine/Pt in CCl_4

solid cinchonidine		on Pt	
IR (cm^{-1})	calc RHF (cm^{-1})	RAIRS (cm^{-1})	description of vibrational mode
1163 (m)	1155	1166 (w)	QB C−H ip bend. + QN CH_2 wag/rock
1180 (w)		1180 (w)	QP ip CH def
1207 (m)	1212	1211 (w)	QN CH_2 torsion and wag + Q C−H ip bend
1238 (w)	1239	1238 (m)	QP ip ring def
1326 (w)	1323	1320 (m)	QB ip ring def + QN CH_2 wag
1336 (w)	1334	1341 (w)	QN CH wag + Q CNC and CCC A stretch
1383 (m)	1381	1382 (w)	Q ring stretch and CH ip bend
1423 (w)	1417	1425 (m)	Q ip ring def
1453 (m)	1466	1439 (m)	QN CH_2 oop scissor
1463 (w)	1478	1463 (vs)	QN CH_2 oop scissors
1508 (m)	1506	1512 (vs)	Q ip ring def + Q C−H ip bend
1569 (m)	1603	1573 (m)	Q ip ring def + Q C−H ip bend
1591 (m)	1619	1592 (m)	Q ip ring def + Q C−H ip bend

interaction between that portion of the molecule and the surface. The IR assignments for the high coverage are summarized in Table 3.

4. Conclusions

A comprehensive set of vibrational band assignments has been developed for the very important chiral modifier cinchonidine. Both Raman and infrared spectra of cinchonidine and related compounds have been presented. The band assignments have been accomplished via the combined use of several methods. These include the use of characteristic frequency tables, spectral comparisons between the parent and fragment molecules, and most importantly, the use of ab initio quantum chemical calculations. Very good agreement between vibrational frequencies was found with both Hartree−Fock and B3PW91 DFT methods when the appropriate scaling factors were used to adjust the raw calculated values. By examining three related conformers of cinchonidine, we determined that variations in the two main dihedral angles in the group linking the quinoline and quinuclidine groups has a negligible effect on localized vibrational bands such as those associated with the quinoline and vinyl groups. The vibrational information has been used to assign the SERS and RAIRS peaks observed in situ for adsorbed cinchonidine on polycrystalline platinum in ethanol and CCl_4 solutions. Using well-established selection rules for both approaches, the adsorption conformations of cinchonidine were determined. At low concentrations, the cinchonidine adsorbs mainly in a "flat" orientation with a strong interaction of the aromatic ring with the platinum surface. As the concentration increases, however, the angle of the quinoline ring with respect to the surface normal increases, and some degree of sigma bonding between the quinoline N atom and the surface becomes apparent. These findings appear to be generally consistent with what has been proposed to occur during the enantioselective hydrogenation reactions that this system is well-known to catalyze.

As the present study demonstrates, even for a molecule as large as cinchonidine, extensive vibrational band assignments may be made using a combination of traditional as well as ab initio approaches. Many molecules with similar complexity have applications as modifiers or ligands in catalytic systems, both homogeneous and heterogeneous, used for fine chemicals and pharmaceuticals production. As such, these results bode well for future bulk and surface vibrational studies of these important systems.

Acknowledgment. This work was funded by the American Chemical Society Petroleum Research Fund (PRF) under Grants No. ACS-PRF#35610-G5 and ACS-PRF#36753-AC. Additional funding was provided by the Department of Energy Award No. DE-FG02-03ER15472-A000. F.Z. also wishes to thank Thomas H. Morton for his help with the RHF calculations.

References and Notes

(1) For a comprehensive review see: Baiker, A. *J. Mol. Catal. A* **1997**, *115*, 473.
(2) Orito, Y.; Imai, S.; Niwa, S. *Collected papers of the 43rd catalysis forum*; Japan, 1978; p 30.
(3) Wang, G.-Z.; Mallat, T.; Baiker, A. *Tetrahedron Asymm.* **1997**, *8*, 2133.
(4) Torok, B.; Felfoldi, K.; Balazsik, K.; Bartok, M. *J. Chem. Soc., Chem. Commun.* **1999**, 1725.
(5) Struder, M.; Burkhardt, S.; Blaser, H.-U. *J. Chem. Soc., Chem. Commun.* **1999**, 1727.
(6) Augustine, R. L.; Setrak, K. T.; Doyle, L. K. *Tetrahedron Asymm.* **1993**, *4*, 1803.
(7) Wells, P. B.; Wilkinson, A. G. *Top. Catal.* **1998**, *5*, 39.
(8) Blaser, H.-U.; Jalett, H.-P.; Garland, M.; Studer, M.; Thies, H.; Wirth-Tijana, A. *J. Catal.* **1998**, *173*, 282.
(9) Wang, J.; Sun, Y.-K.; LeBlond, C.; Landau, R. N.; Blackmond, D. G. *J. Catal.* **1996**, *161*, 752.
(10) Sun, Y.-K.; Wang, J.; LeBlond, C.; Landau, R. N.; Blackmond, D. G. *J. Catal.* **1996**, *161*, 759.
(11) LeBlond, C.; Wang, J.; Andrews, A. T.; Sun, Y.-K. *Top. Catal.* **2000**, *13*, 169.
(12) Carley, A. F.; Rajumon, M. K.; Roberts, M. W.; Wells, P. B. *J. Chem. Soc., Faraday Trans.* **1995**, *91*, 2167.
(13) Bonello, J. M.; Lambert, R. M. *Surf. Sci.* **2002**, *498*, 212.
(14) Xu, Q. M.; Wang, D.; Wan, L. J.; Bai, C. L.; Wang, Y. *J. Am. Chem. Soc.* **2002**, *124*, 14300.
(15) Kubota, J.; Zaera, F. *J. Am. Chem. Soc.* **2001**, *123*, 11115.
(16) Kubota, J.; Ma, Z.; Zaera, F. *Langmuir* **2003**, *19*, 3371.
(17) Zaera, F. *Int. Rev. Phys. Chem.* **2002**, *21*, 433.
(18) Ma, Z.; Kubota, J.; Zaera, F. *J. Catal.* **2003**, *219*, 404.
(19) Ferri, D.; Bürgi, T.; Baiker, A. *J. Chem. Soc., Chem. Commun.* **2001**, 1172.
(20) Ferri, D.; Bürgi, T. *J. Am. Chem. Soc.* **2001**, *123*, 12074.
(21) Ferri, D.; Bürgi, T.; Baiker, A. *J. Catal.* **2002**, *210*, 160.
(22) Chu, W.; LeBlanc, R. J.; Williams, C. T. *Catal. Commun.* **2002**, *3*, 547.
(23) LeBlanc, R. J.; Chu, W.; Williams, C. T. *J. Mol. Catal. A*, in press.
(24) Socrates, G. *Infrared and Raman Characteristic Group Frequencies: Tables and Charts*, 3rd ed.; Wiley: Chichester, U.K., 2001.
(25) Lin-Vien, D.; Colthup, N. B.; Fateley, W. G.; Grasselli, J. G. *The Handbook of Infrared and Raman Characteristic Frequencies of Organic Molecules*; Academic Press: San Diego, 1991.
(26) Weselucha-Birczynska, A.; Nakamoto, K. *J. Raman Spectrosc.* **1996**, *27*, 915.
(27) Yoon, T. P.; Jacobsen, E. N. *Science* **2003**, *299*, 1691.
(28) Frisch, M. J.; Trucks, G. W.; Schlegel, H. B.; Scuseria, G. E.; Robb, M. A.; Cheeseman, J. R.; Zakrzewski, V. G.; Montgomery, J. A., Jr.; Stratmann, R. E.; Burant, J. C.; Dapprich, S.; Millam, J. M.; Daniels, A. D.; Kudin, K. N.; Strain, M. C.; Farkas, O.; Tomasi, J.; Barone, V.; Cossi, M.; Cammi, R.; Mennucci, B.; Pomelli, C.; Adamo, C.; Clifford, S.; Ochterski, J.; Petersson, G. A.; Ayala, P. Y.; Cui, Q.; Morokuma, K.; Malick, D. K.; Rabuck, A. D.; Raghavachari, K.; Foresman, J. B.; Cioslowski, J.; Ortiz, J. V.; Baboul, A. G.; Stefanov, B. B.; Liu, G.; Liashenko, A.; Piskorz, P.; Komaromi, I.; Gomperts, R.; Martin, R. L.; Fox, D. J.; Keith, T.; Al-Laham, M. A.; Peng, C. Y.; Nanayakkara, A.; Challacombe, M.; Gill, P. M. W.; Johnson, B.; Chen, W.; Wong, M. W.; Andres, J. L.; Gonzalez, C.; Head-Gordon, M.; Replogle, E. S.; Pople, J. A. *Gaussian 98*, revision A.9; Gaussian, Inc.: Pittsburgh, PA, 1998.
(29) Becke, A. D. *J. Chem. Phys.* **1993**, *98*, 5648.
(30) Perdew, J. P.; Wang, Y. *Phys. Rev. B* **1992**, *45*, 13244.
(31) Perdew, J. P.; Chevary, J. A.; Vosko, S. H.; Jackson, K. A.; Pederson, M. R.; Singh, D. J.; Fiolhais, C. *Phys. Rev. B* **1992**, *46*, 6671.
(32) Hay, P. J.; Wadt, W. R. *J. Chem. Phys.* **1985**, *82*, 270.
(33) Wadt, W. R.; Hay, P. J. *J. Chem. Phys.* **1985**, *82*, 284.
(34) Hay, P. J.; Wadt, W. R. *J. Chem. Phys.* **1985**, *82*, 299.
(35) Scott, A. P.; Radom, L. *J. Phys. Chem.* **1996**, *100*, 16502.
(36) Halls, M. D.; Velkovski, J.; Schlegel, H. B. *Theor. Chem. Acc.* **2001**, *105*, 413.
(37) Pople, J. A. *Rev. Mod. Phys.* **1999**, *71*, 1267.
(38) Schaftenaar, G.; Noordik, J. H. *J. Comput.-Aided Mol. Design* **2000**, *14*, 123.
(39) Bode, B. M.; Gordon, M. S.*J. Mol. Graph. Mod.* **1999**, *16*, 133.
(40) Wait, S. C.; McNerney, J. C. *J. Mol. Spectrosc.* **1970**, *34*, 56.
(41) Bandyopadhyay, I.; Manogaran, S. *Indian J. Chem.* **2000**, *39A*, 189.
(42) Bruesch, P. *Spectrochim. Acta* **1966**, *22*, 867.

(43) Bruesch, P.; Guenthard, H. H. *Spectrochim. Acta* **1966**, *22*, 877.
(44) Katritzky, A. R.; Jones, R. A. *J. Chem. Soc.* **1960**, 2942.
(45) Oleksyn, B. J.; Suszko-Puzycka, A.; Dive, G.; Lamotte-Brasseur, J. *J. Pharm. Sci.* **1992**, *81*, 122.
(46) Buergi, T.; Baiker, A. *J. Am. Chem. Soc.* **1998**, *120*, 12920.
(47) Ferri, D.; Bürgi, T.; Baiker, A. *J. Chem. Soc., Perkin Trans. 2* **1999**, 1305.
(48) Margitfalvi, J. F.; Tfirst, E. *J. Mol. Catal. A* **1999**, *139*, 81.
(49) Aranda, D. A. G.; Carneiro, J. W. M.; Oliveira, C. S. B.; Passos, F. B.; Souza, P. R. N.; Antunes, O. A. C. *Brazilian J. Chem. Eng.* **2001**, *18*, 287.
(50) Stewart, J. J. P. *J. Comput. Chem.* **1989**, *10*, 209.
(51) Stewart, J. J. P. *J. Comput. Chem.* **1989**, *10*, 221.
(52) Oleksyn, B. J. *Acta Crystallogr.* **1982**, *B38*, 1832.
(53) Palafox, M. A. *Int. J. Quantum Chem.* **2000**, *77*, 661.
(54) Weselucha-Birczynska, A.; Nakamoto, K. *J. Mol. Struct.* **2000**, *555*, 391.
(55) Woon, D. E.; Dunning, T. H., Jr. *J. Chem. Phys.* **1993**, *98*, 1358.
(56) Bolboaca, M.; Kiefer, K.; Popp, J. *J. Raman Spectrosc.* **2002**, *33*, 207.
(57) Greenler, R. G. *J. Chem. Phys.* **1966**, *44*, 310.
(58) Zaera, F. In *Encyclopedia of Chemical Physics and Physical Chemistry*; Moore, J. H., Spencer, N. D., Eds.; IOP Publishing Inc.: Philadelphia, 2001; Vol. 2, p 1563.
(59) Zaera, F.; Hoffmann, H.; Griffiths, P. R. *J. Electron Spectrosc. Relat. Phenom.* **1990**, *54*/*55*, 705.
(60) Creighton, J. A. *Surf. Sci.* **1983**, *124*, 209.
(61) Moskovitz, M. *J. Chem. Phys.* **1982**, *77*, 4408.
(62) Moskovitz, M.; Suh, J. S. *J. Phys. Chem.* **1984**, *88*, 1293.
(63) Creighton, J. A. in *Spectroscopy of Surfaces*; Clark, R. J. H., Hester, R. E., Eds.; John Wiley and Sons: New York, 1988; p 37.
(64) Zou, S.; Williams, C. T.; Chen, E. K.-Y.; Weaver, M. J. *J. Phys. Chem. B* **1998**, *102*, 9039.
(65) Cai, W. B.; She, C. X.; Ren, B.; Yao, J. L.; Tian, Z. W.; Tian, Z. Q. *J. Chem. Soc., Faraday Trans.* **1998**, *94*, 3127.
(66) Yao, J.-L.; Ren, B.; Liu, G.-K.; Wu, D.-Y.; Gu, R.-A.; Tian, Z. Q. *J. Raman Spectrosc.* **2003**, *34*, 221.
(67) Chowdhury, J.; Ghosh, M.; Misra, T. N. *Spectrochim. Acta A* **2000**, *56*, 2107.
(68) Zawada, K.; Bukowska, J. *Surf. Sci.* **2002**, *507*−*510*, 34.
(69) Zawada, K.; Bukowska, J. *J. Mol. Struct.* **2000**, *555*, 425.
(70) Kudelski, A.; Pettinger, B. *Chem. Phys. Lett.* **2000**, *321*, 356.
(71) Tuinstra, F.; Koenig, J. L. *J. Chem. Phys.* **1970**, *53*, 1126.
(72) LeBlond, C.; Wang, J.; Liu, J.; Andrews, A. T.; Sun, Y. K. *J. Am. Chem. Soc.* **1999**, *121*, 4920.